Geophysical Approach in the Geological Characterization of Chebabta Dam, Northeast-Algeria

Hocine Benhammadi, Djamel Boubaya*

Water and Environment Laboratory, Department of Earth and Planetary Sciences, Larbi Tebessi University, Constantine st. 12002, Tebessa, Algeria

Layachi Gouaidia

Sedimentary Environment Laboratory, Mineral and Water Resources of Eastern Algeria, Department of Earth and Planetary Sciences, Larbi Tebessi University, Constantine st. 12002, Tebessa, Algeria

Hicham Chaffai

Laboratory of Water Resources and Sustainable Development (REDD), Department of Geology, Faculty of Earth Sciences, University Badji Mokhtar, PO Box 12, 23000, Annaba, Algeria

*Corresponding author: djamel.boubaya@gmail.com; d.boubaya@univ-tebessa.dz

Meskiana Area is characterized by a semi-arid climate, where water supply for irrigation and industry is not sufficient as the priority goes for domestic use. To meet the increasing population growth and development, the authorities have considered building a new water retaining structure on some major temporary water streams. For this purpose, Chebabta Site on Meskiana Wadi was chosen as the future dam site. It is large enough to store the desired volume of water.

This study investigates the conditions of the site and the adequacy of the ground as a foundation for the project-ed dam. The conditions of the site include the geological structure and mainly the presence of discontinuities in the formation on which the dam will be built, the nature of the lithologies under the foundation and the future lake, and the presence of any hazard. This site characterization is usually carried out using different methods in order to highlight any underground buried problematic structure. In this context, the different geophysical techniques remain the most used ones. Four geophysical methods were used in the case of Chebabta dam site, namely seismic refraction, constant separation traversing (CST), vertical electric sounding (VES) and electric

resistivity tomography (ERT). The choice of the techniques and the location of the survey lines was made on the basis of the available geological data. In this sense, profiles were established on both banks of Meskiana Wadi.

The obtained results allowed a better characterization of the geological structure, defining the limit between the surface cover and the bedrock, which is, in other words, the limit between the weathered zone and the bedrock. Their respective thicknesses were also determined by seismic refraction and VES. However, ERT succeeded in estimating the thickness of alluvial deposits in the left bank of the Wadi and positioning a fault structure passing at the east of the study area.

Introduction

The lack of a clear picture of the underground geological structures, whatever their type may be, constitutes a major hazard for development projects, property and the people (Benson et al., 1998). Therefore, it is necessary to carry out a site investigations survey for detection and recognition of the buried structures, before any construction is laid out. In general, the overall procedure is organized in the context of three major site reconnaissance phases. The preliminary phase is usually dedicated to office study, where all previous works and available data in the area are reviewed. In this phase, the subsoil conditions which may constitute a threat to the performance of the structure are revealed and must be clarified by more appropriate methods in the detailed investigation stage.

The detection of underground structures by an indirect method mainly includes the realization of investigations by means of one or more geophysical methods. They allow the analysis and recognition of a site even before the installation of a construction work (Lagabrielle, 2007). The appropriate methods depend on the characteristics of the site and the development project (size, depth, filling, etc.). Geophysical measurements provide an image of the geological layers of the basement, the interpretation of which leads to the detection of geophysical anomalies that may be due to the presence of underground geological faults (*Fig. 1*).

Recently, near the study area, based on the geographic information system (GIS) and remote sensing (RS) techniques, Mahleb et al. (2022) have adapted the Revised Universal Soil Loss Equation (RUSLE) model to map the spatial distribution of soil erosion susceptibility of Meskiana Watershed. Several geophysical studies have been used for the characterization of dam sites. For example, Gouasmia et al. (2007) have used an integration of seismic refraction and VES to study the Oum Leksab dam in Tunisia. Sari et al. (2020) have given a detailed review of the use of geophysical methods for dam site characterization.

The objectives common to the site of the Chebabta Dam are to define precisely the lithological nature and the geological structure of the formations (surface cover/bedrock, thickness of alluvium, and position of the F1 fault), which constitute the foundation of the dam. In addition to the three geophysical methods carried out within the framework of the project, namely seismic refraction, electric profiling and vertical electric sounding, with the aim of better characterizing the site, we carried out an electric resistivity tomography survey, a technique of imaging the subsoil based on the measurement of apparent resistivities (Zhou et al., 2002). In this article, the case study of the dam is discussed to demonstrate the contribution and usefulness of geophysical methods as a tool for the characterization and identification of underground hidden structures.

Geographical and climatic context

Meskiana Basin extends over 1680 km² and is located in the northeast of Algeria, 80 km from the Algerian-Tunisian border and 250 km south of the Mediterranean Sea. It is in fact a sub-basin of a greater basin called Mellègue Wadi. From the hydrographic point of view, the basin is drained by a single main watercourse, which is Meskiana Wadi (*Fig. 1*).

Fig. 1. *Situation map of the study area on a Google map showing geophysical lines and the measurement points*
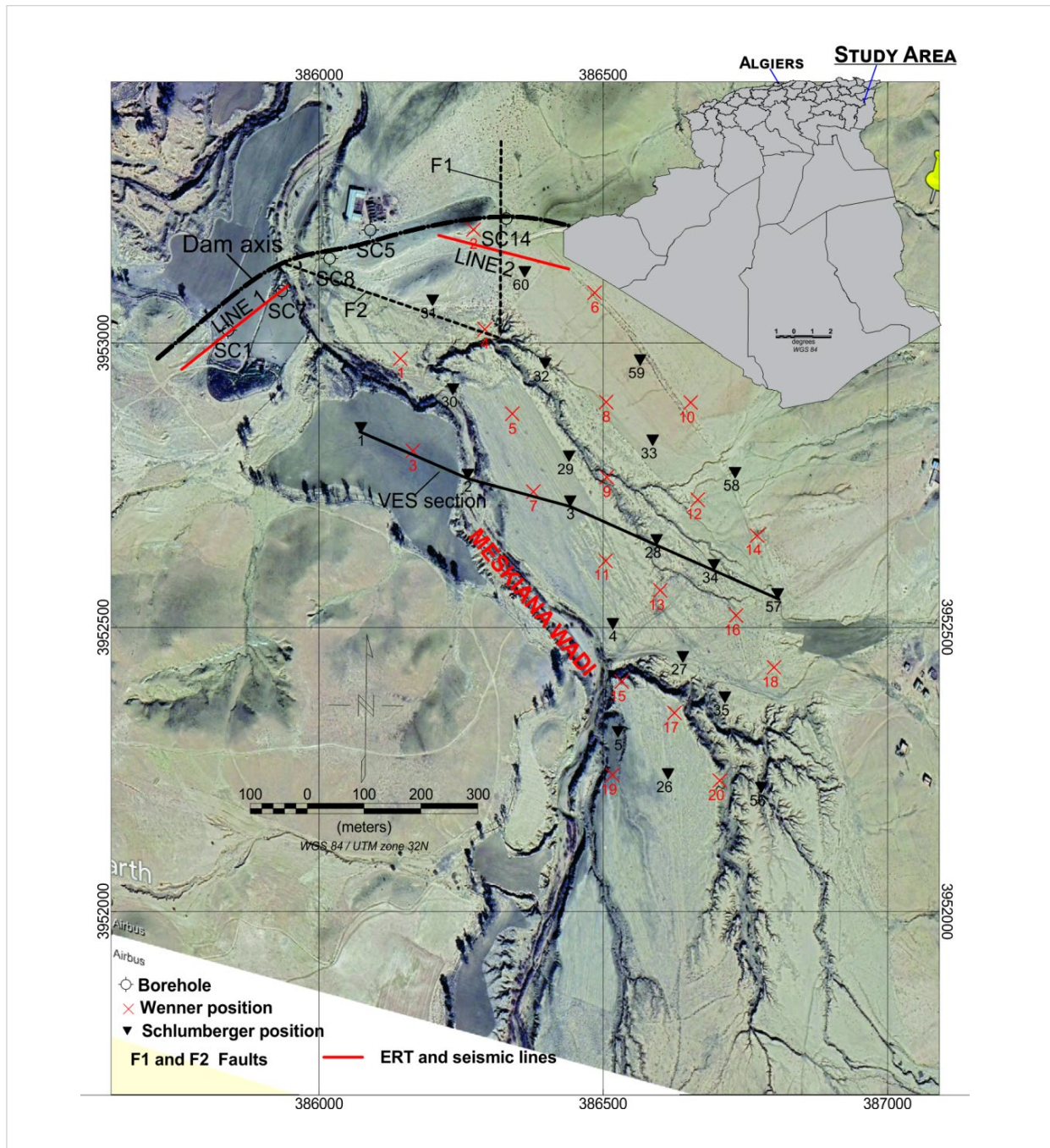
It is considered the main water course that gathers runoff waters flowing over the banks. The climate of the study area is of a semi-arid Mediterranean type, with a cold and rainy winter, and a hot dry summer. The average annual temperature is 15.6°C. The average annual rainfall, over a period of 33 years (1972 – 2005), is estimated around 341 mm.

Geomorphology

The geomorphology of the site and its surroundings is marked by (ANBT, 2018):

1 Large plateaus on the borders of the valley and the site at 800–810 m elevation, that are composed of limestone crusts and puddingstones which are strongly cut by the second-order hydrographic network;

2 Long and gentle slopes carved out of the marl (3% to 5%) locally presenting the relief pattern characteristic of the Bad Lands;

3 A flat and wide valley bottom (150 to 300 m) crowded with recent alluvium;

4 A re-digging of the alluvial deposits at the bottom of the Wadi in the form of a very active regressive dendritic network; this digging can reach 5 to 10 m in depth and defines a minor bed 30 m wide on average; this erosion frequently penetrates the marly bedrock;

5 A long limestone ridge that intersects the valley from bank to bank and marks the "lock" used for the dam.

In the Basin of the future reservoir, the tributaries of the Meskiana wadi form a hairy hydrographic network, the paths of which are influenced by the tender nature of the drained land and the presence of impermeable marly bedrock.

Geological Setting

Meskiana Wadi crosses a vast plain covered with Quaternary deposits, with numerous limestone mounds. The stream bed is dug in the Cretaceous formations covered by the Quaternary. The proposed site for the embankment is located near the Turonian- Cenomanian Boundary (*Fig. 2*).

The site geology is composed from top to bottom (ANBT, 2018) as follows.

Surface formations (Fs). The surface formations include colluvium of slopes, scree, limestone crusts and silts of puddingstones, sandstone and gravel in discontinuous topping on the plateaus, seen on the left bank of the basin.

Alluvium (0A). The Alluvium 0A is designated "undifferentiated alluvium", where the detail is not available. However, at some places of the site, we can differentiate three units of Alluvium 0A:

Alluvium A1: A dark beige brown top set with 2 to 3 m thickness.

Alluvium A2: A light beige brown intermediate set with 2 to 3 m thickness

Alluvium A3: A gravelly base set with 0.5 to 2 m thickness.

Upper marls (1M). Belonging to the Upper Turonian, these gray marls are encountered downstream of the site. Their maximum thickness is undetermined: however, it can be estimated at one to several tens of meters at the project level, especially downstream.

Upper limestone ridge (2C). White gray limestone from the middle Turonian is the upper level of the topographic closing ridge. Their thickness is 10 to 15 m.

Intercalated marls (3M). The 3M Marls are of Turonian age. These dark gray marls are flaky. They form the marly weakness within the topographic ridge, with a thickness of 10 to 16 m.

Lower limestone ridge (4C). Massive gray limestone belonging to the Middle Turonian at the base of the topographic ridge, with the thickness of 10 to 12 m, is not always easy to determine due to more or less rapid transition to the base marls.

Basic marls (5M). A significant thickness of marls and dark gray clayey marls, constitutes the substrate of the project. The (5M) includes: (1) the lower Turonian marls at the base of the lower limestone ridge; (2) intercalated limestone passages; and (3) the Cenomanian mass of similar facies, more clayey in depth with a greenish facies.

The dip of the formations is downstream (15 to 33° towards the NNW). There are three faults on the studied site. The F1 and F2 faults will be discussed later in this article. While, the F3 fault is hypothetical and has no impact on the project.

Hydrogeology

The site area is poor in groundwater reserves. Marls in general are impermeable and only contain a very weak aquifer. Highly fractured limestones are more favorable to the accumulation of groundwater; however, the piezometry shows the presence of a weak static level, probably because of the thinness of the limestone layers.

Fig. 2. *Simplified geologic map of the study area (ANBT, 2018)*
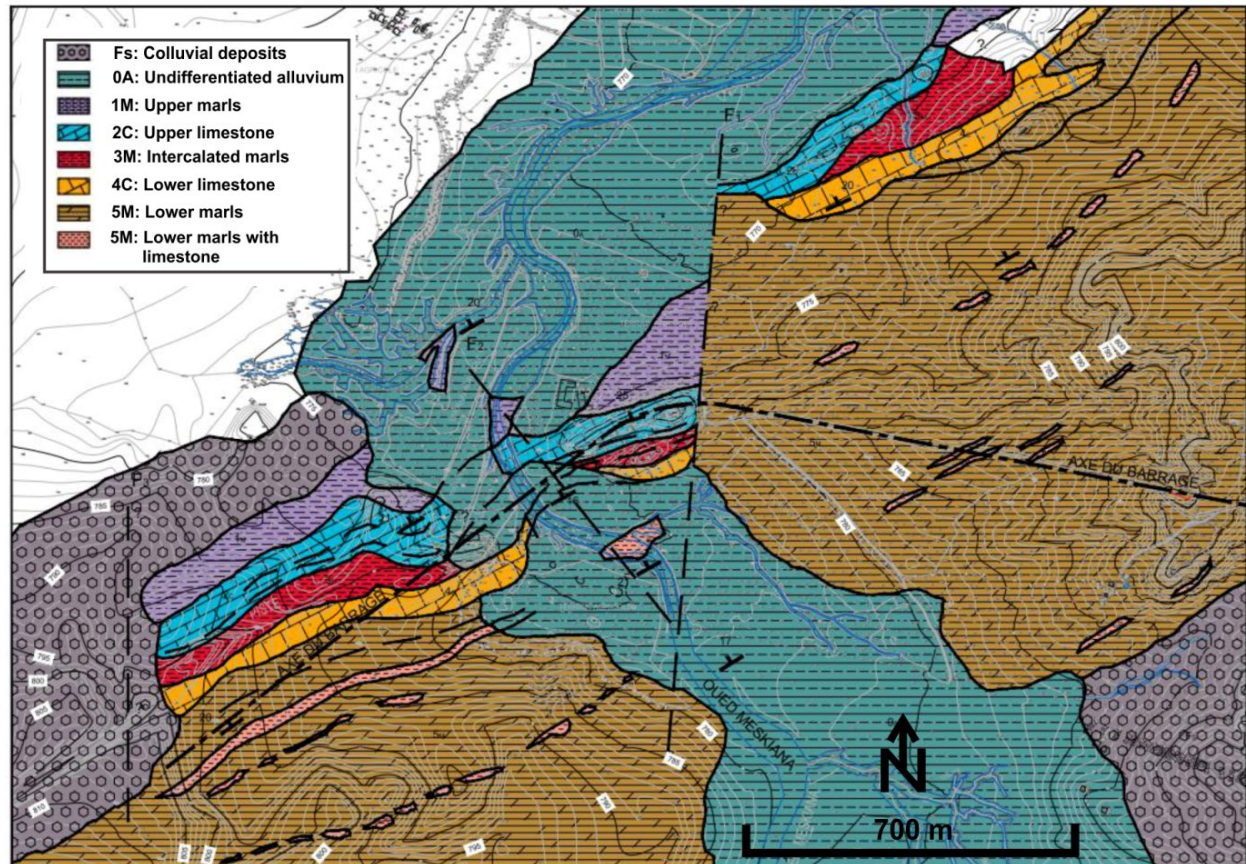
Most of the water resources for the inhabitants are provided by tanks. In addition, the water from the wells would be unfit for consumption because it is too loaded with mineral salts.

The level of the water table is located in the horizon of the weathered base marls (5M) and follows the general dip of the layers towards the Wadi. The variations of the water table are also very small. In the centre of the site, the level of the water table is generally between 766 and 767 m, which corresponds to the level of the wadi. These findings confirm that the water table is drained by the Wadi and acknowledge the general impermeability of the site and the basin.

Materials and methods

The prospecting campaign by geophysical methods took place in December 2016 (Yousfi & Douaifia, 2020).

A geophysical study using three methods, namely seismic refraction, CSTor Electric Profiling and VES. ERT was performed by our team on November 2020. These geophysical methods were designed for the characterization of the site and defining the limit between the surface cover and the unweathered rock.

Seismic refraction

The seismic refraction method makes it possible to determine the nature and depth of the bedrock. The principle of the seismic refraction method is based on the calculation of the travel time curve of direct and refracted seismic waves.

The seismic refraction survey was carried out using the SUMMIT XStream Pro (DMT) with 10 Hz vertical geophones and sets of 24-channel spread cables. Measurements and parameters for seismic data recording are controlled by the "SUMMIT Acquisition

Tool NET". All recording and shooting parameters that are necessary for seismic data acquisition are defined in the "Recording Parameters" and "Shooting Parameters" windows of the software (Summit XStream Pro user guide, 2015).

The seismic refraction data was acquired along two lines or profiles over 2 spreads for each line, and saved in SEG2 format. With the 5 m geophone spacing, the length of each spread for the 24 channel is 115 m. Each line was measured independently with one overlapping geophone resulting in a continuous profile covering about 230 m distance.

For each seismic data acquisition,7 hammer-shots were fired: at 30 m from the first geophone (direct off-set shot), a direct end shot 2.5 m before geophone 1, an intermediate shot between geophones 6 and 7, a central shot between geophones 12 and 13, an intermediate shot between geophones 18 and 19, an end reverse shot 2.5 m after geophone 24, and a reverse off-set shot at 30 m from geophone 24.

Seismic data interpretation was done using WinSism V10 software (W-Geosoft, 2004). This software makes it possible to pick first breaks on the "screen", to assemble the travel time curves as well as to perform graphically all the usual operations translation of the traces, calculation of the intercept times, thicknesses computation and plotting of the seismic profile.

Constant Separation Traversing (CST) or Electric Profiling

CST or Electric Profiling uses a manual electrode array, in which the electrode separation is kept fixed (Reynolds, 2011). This makes it possible to study the change of resistivity in the horizontal or lateral direction. In our case, the Wenner array was used. For this array, the four electrodes are collinear and are equally spaced. The receiving electrodes (M, N) are between the current electrodes (A, B).

The entire array is moved along the profile, and values of apparent resistivity at the centre of the array are recorded. The CST method is used to highlight anomalous zones with either high or low apparent resistivity values.

For each CST station, two separations were used, namely AB = 15 m and AB = 45 m on an irregular grid. In total, 20 CST points were collected to evaluate the thickness of the infill materials at the borrow zone.

Vertical Electrical Sounding (VES)

VES shows how resistivity varies with depth, assuming no lateral variation of resistivity. In the VES method, the positions of the electrodes are changed with respect to a fixed point known as the sounding point. In this way, the measured resistance values at the surface reflect the vertical distribution of resistivity values in a geological section. The VES procedure consists of passing a known amount of current (I) into the ground through two current electrodes, A and B, and measuring the potential difference (V) developed between the potential electrodes M and N. The spacing between the current electrodes is gradually increased while the distance between potential electrodes is increased only when the observed potential difference across M and N becomes quite low (Singh et al., 2011).

The system used for electrical soundings is the SARIS (Scintrex Automated Resistivity Imaging System) with: (1) AB and MN wiring, (2) stainless steel electrodes 55 cm long and 1.4 cm in diameter and (3) a power supply (12V battery).

The IPI2Win software was used for inverting the resistivity soundings. This software performs an automated inversion of the initial resistivity model using the observed data. IPI2Win uses a linear filtering approach for the forward modelling, and the inversion is achieved by a regularized optimization based on Tikhonov's approach (Bobachev, 2002). It works on an iterative mode by giving at the end of each step: (a) an updated model of layer thickness and true resistivity and (b) the misfit function (RMS) between observed apparent resistivity and calculated apparent resistivity. The starting model used during the inversion for each VES consisted of three to four layers, and layering thickness was constrained using known geology and lithology from nearby boreholes.

The electric soundings were of the Schlumberger type (ABmax from 60 to 400 m). A total of 20 VES points were collected to evaluate the thickness of the infill materials at the borrow zone and the depth to the bedrock.

Electrical Resistivity Tomography (ERT)

For a better geological characterization of the site, the ERT technique was conducted by our team in November 2020. The choice of this method is motivated

by the shallow depth of seismic investigations and characterization of F1 fault at the eastern part of the study area.

The ERT method has been widely used as a reconnaissance tool in groundwater and environmental studies because it yields a good correlation between a terrain's electrical resistivity and its geology and fluid content with numerous successful case histories (Boubaya et al., 2017; Mouici et al., 2017; Fehdi et al., 2011). Two 235-m long electrical resistivity tomography lines were carried out using the multi-node switching system SYSCAL-Pro resistivity meter (IRIS-Instruments, Orleans, France). The system is composed of 48 electrodes, that enabled the automatic measurements of apparent resistivity using a Wenner-Schlumberger configuration with an electrode spacing of 5 m. The recorded apparent resistivity data were saved on the memory of the resistivity meter and then transferred to an external PC for further processing and interpretation. For our system of 48 electrodes and a Wenner-Schlumberger array, the median depth of investigation (Loke, 2012) is equal to 47 m considering an electrode spacing of 5 m. The ERT data were processed to generate 2D resistivity models using Res2dinv 2D resistivity inversion software (Loke & Barker, 1996).

Results and Discussion

The obtained results from the four geophysical techniques are as follows.

Seismic refraction

The refraction seismic, which concerned the upper part (0 to 15 m) of the geological section, made it possible to detect 2 to 3 layers. The first two layers generally correspond to alluvium or weathered rocks. The deep layer characterizes the bedrock or unweathered rocks. The location of the interpreted seismic sections is shown in *Fig. 1*.

The seismic section of line 1 or profile 1 (*Fig. 3*), on which are shown the boreholes SC-1 and SC-7, made it possible to highlight 2 seismic layers on its SW part and 3 layers on its NE part. The interpretation of this profile is based on the comparison with borehole lithology. The SW part with 2 seismic layers shows a near surface layer with velocities (720–870 m/s) and an average thickness of 6 m corresponding to alluvium (0A). The second layer correlates with marly bedrock (3M) having seismic velocities between 2473 and 3300 m/s. For the NE part of the profile with 3 layers, we note, respectively, a first layer with seismic velocity 360–518 m/s and an average thickness of 2 m that

Fig. 3. *Seismic section of line 1 at the left bank of the Wadi*
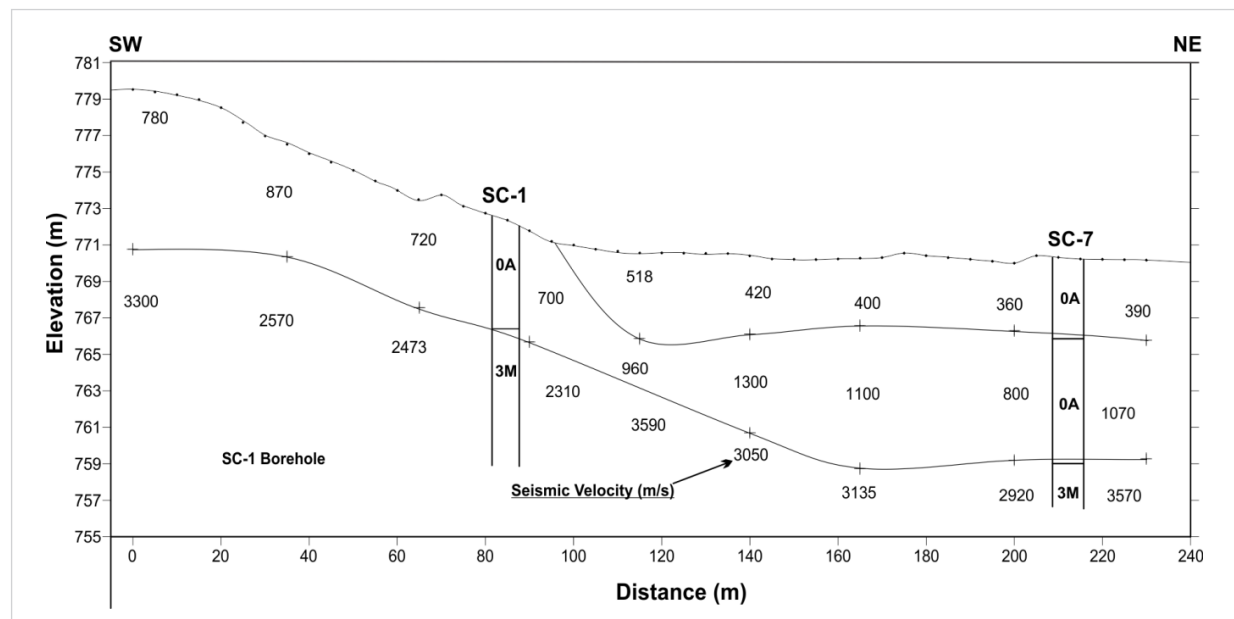
correlates with the upper part of the alluvium (0A). Then an intermediate layer having seismic velocities between 700 and 1300 m/s and thickness of the order of 6 m that correlates with the lower part of the alluvium (0A). The bedrock corresponds to marls (5M) with velocities ranging from 2310 to 3590 m/s.

The seismic section of line 2 (*Fig. 4*) is situated in the eastern part of the study area. This line is interpreted with 3 seismic layers: the first layer with 2 to 4 m thick and low velocities (400–530) corresponding to collivium; the second layer corresponding in the left of the borehole SC-14 to weathered limestone (4C) and to the right of the borehole SC-14 to weathered marls (1-5M); the deep layer corresponding to unweathered limestone (4C) and marls (2-5M). A thickening of the second weathered layer near the borehole SC-14 is probably caused by the F1 fault. As we can see, the exact position of the F1 fault is not well recovered by the seismic refraction method. This prompted us to use the electrical tomography method that clearly highlighted the F1 fault as we will see later.

Resistivity maps (Wenner AB = 15 m and Schlumberger AB = 14 m)

The apparent resistivity values of the Wenner AB = 15 m and Schlumberger AB = 14 m arrays corresponding to the centre of each array were gridded and plotted on a map. These two maps correspond to an investigation depth of about 3 m (*Fig. 5*). The apparent resistivities as shown on the colour bar are low (between 4 and 49 ohm-m). The objective of these two maps is the highly conductive layer (apparent resistivity less than 8 ohm-m blue colour) which corresponds to the clay material. These two maps give approximately the same results; however, the Schlumberger map indicates less high resistivity values compared with the Wenner map. The relatively high values of the apparent resistivities correspond to marls, while the lowest represent clays. The resistivity ranges above 8 ohm-m mark the absence or the low thicknesses of the highly conductive clay formation. Both maps highlight a potential area for clayey alluvium (0A).

Resistivity maps (Wenner AB = 45 m and Schlumberger AB = 40 m)

The colour bar is the same as for the previous maps. These two maps correspond to an investigation depth of about 8 m. From a depth of about 8 m, the apparent resistivities start to rise (*Fig. 5*). The environment becomes relatively resistant (marly), which is in agreement with the borehole data.

In general, the site is characterized by low resistivities showing that the geological formations are impermeable.

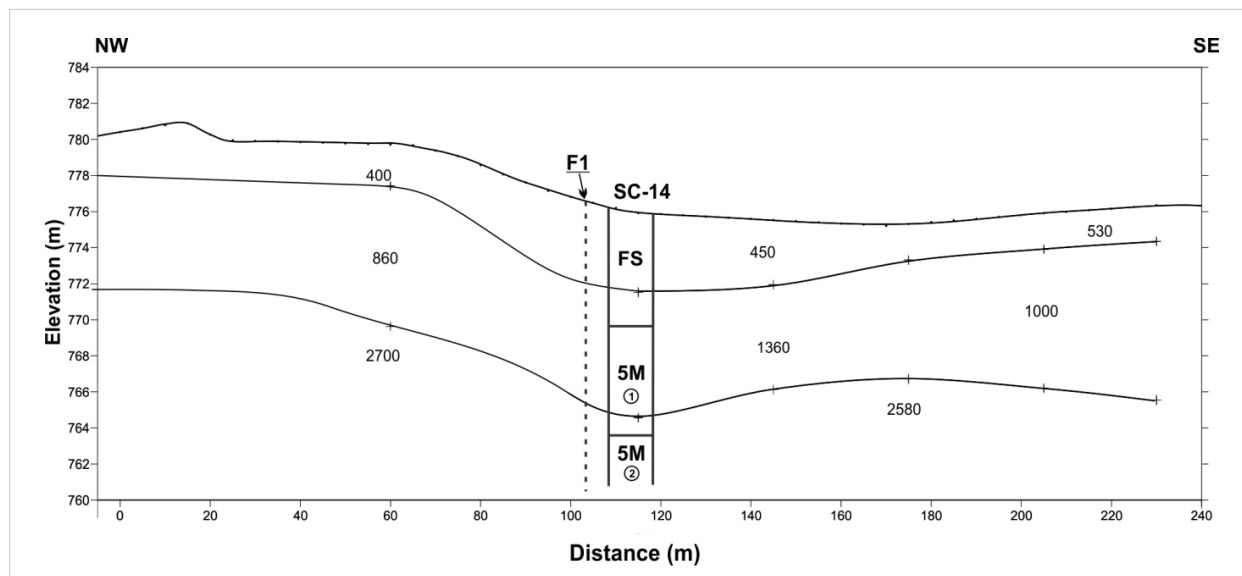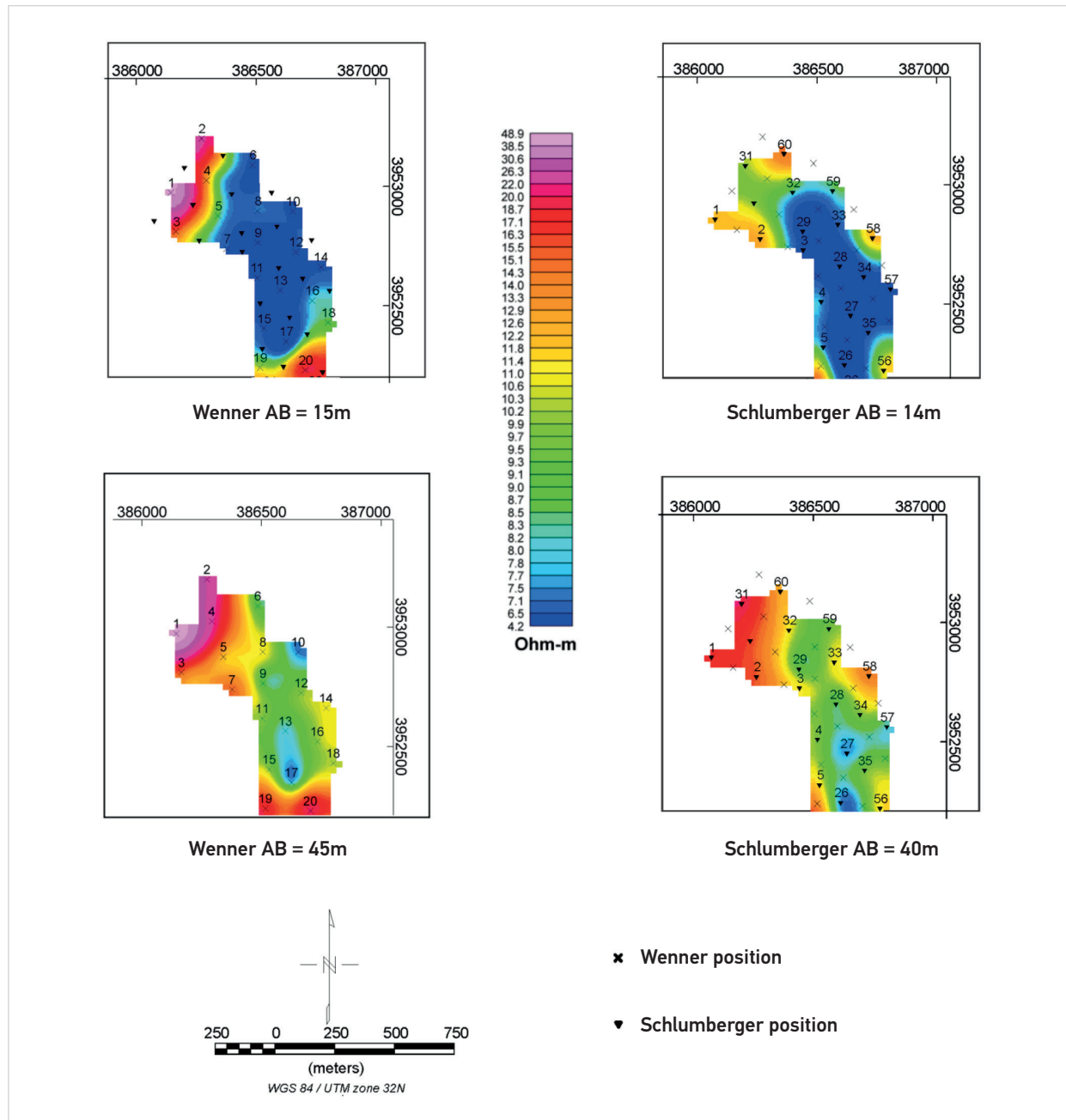**Fig. 4.** *Seismic section of line 2 at the East of the study area (for legend see Fig. 3)*

Fig. 5. *Resistivity maps of the Wenner and Schlumberger arrays (see Fig. 1 for station locations)*

## Vertical Electrical Sounding (VES)

The result of the correlation of six VES is shown in *Fig. 6*. The upper panel of the figure shows the VES curves, where as the bottom panel shows the geo-electric section. True interpreted resistivity values are indicated by numbers inside layers and by grey colour. The shapes of the VES sounding curves are of H type except the last one which has an HK type. The geoelectric section is interpreted, from top to bottom, as follows: (1) a near surface layer that corresponds to agricultural soil (0A) with resistivity in

Fig. 6. *Geo-electric section from the quantitative interpretation of VES data in terms of 1D model (VES stations and geo-electric line are shown in Fig. 1)*
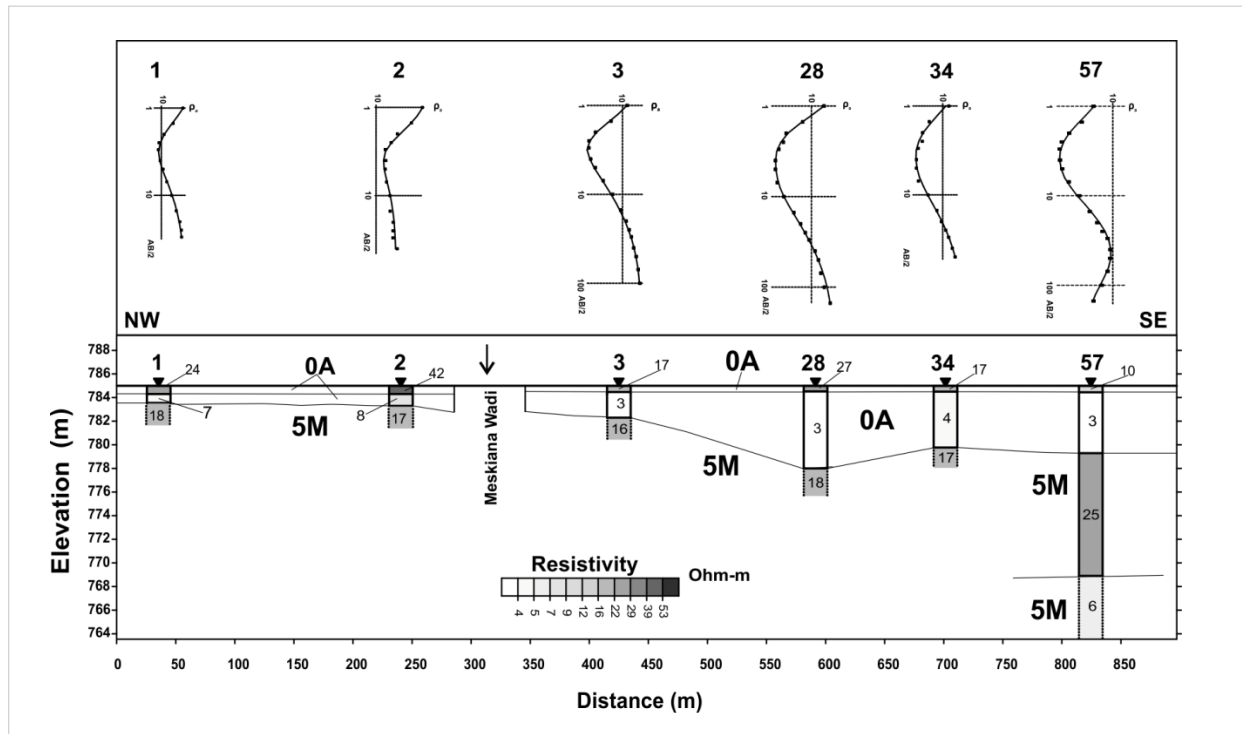
the range 10–42 ohm-m and thickness of 0.5–0.6 m; (2) a clayey layer (0A) with resistivities in the range 3–7 ohm-m and thickness 2–6 m; the second layer that is present on all VES curves shows a high potential for clay infill material and is relatively more conductive and thick at the right bank of the Wadi, below soundings 3, 28, 34 and 57; (3) a marly layer (5M) with resistivities in the range 16–25 ohm-m; and (4) a conductive marly layer (5M) with resistivity of 6 ohm-m is also seen under the last VES. The summary of the interpretation of VES curves of the geo-electric section of *Fig. 6* representing layer thicknesses and true resistivities is shown on *Table 1*.

Low resistivity values of the second conductive layer confirm that alluvium is essentially made up of fine materials (clay and silt).

Alluvial deposits that fill the valley correspond to lacustrine-type deposits and therefore set up within a water body. There was at a remote time a natural basin probably closed either at the level of the site or further downstream in which the fine sediments were deposited in a very uniform way.

Table 1. *Summary of the interpretation of VES curves of the geo-electric section of Fig. 6*

VES number	AB max	Curve Type	Layer number	Resistivity (Ohm-m)	Thickness (m)
1	60	H	1	24	0.6
			2	7	2
			3	18	–
2	80	H	1	42	0.8
			2	8	1.6
			3	17	–
3	200	H	1	17	0.6
			2	3	2
			3	16	–
28	300	H	1	27	0.5
			2	3	6
			3	18	–
34	100	H	1	17	0.5
			2	4	5
			3	17	–
57	300	HK	1	10	0.6
			2	3	5
			3	25	10
			4	6	–

It is concluded that the basin area has already functioned as a lake, which is encouraging for its water-tightness.

Electric Resistivity Tomography

The ERT data were processed to generate 2D resistivity models. The inversion procedure for the two electrical tomography lines converged to an RMS error of 2.4% and 4.9% between measured and calculated apparent resistivity. ERT lines are shown in *Fig. 1*.

ERT (Line 1)

The resistivity inverted section of line 1 with the locations of the boreholes SC-3 and SC-7 also marked on it is shown in *Fig. 7*. There is a good correlation between the location of the low resistivity zone and the alluvium 0A. This significant accumulations of low-resistivity material (between mark 120 to the end of the line) indicates the promising potential for infill material. A comparison of the inverted resistivity section and borehole SC-7 shows that the thickness (about 10 m) and the depth of the infill material (alluvions), mapped by the ERT survey, is in good agreement with the results of drilling. The deep parts of the resistivity section are dominated by high resistivities corresponding to limestone ridge (4C). It seems that the deep 5M marls were not detected by the set of 48 electrodes with 5 m electrode interval and Wenner-Schlumberger array.

It should be noted, however, that there is a resistant inversion artefact below station or mark 120, located approximately in the centre of the line at 5 m depth.

ERT (Line 2)

The ERT results show that the F1 fault (*Fig. 8*) is marked by a rapid change of resistivity between high resistivity limestone (4C) and low resistivity marls (5M). It is located approximately at mark 107 left of the projection of borehole SC-14 on the ERT line. The borehole SC-14 indicated from top to bottom: (1) colluvial deposits (FS), (2) weathered lower marls (1-5M), (3) lower marls (2-5M) and (4) lower marls with limestone (3-5M).

The left strike sleep fault F1 puts in contact the thick marly series 5M in its Eastern part with the succession 1M-2C-3M-4C in its Western part (see *Fig. 2*). The 1M-2C-3M-4C formations in the NE part are shifted by the F1 towards the north.

Borehole SC14, tilted towards the west, was intended to intersect the fault F1. Nevertheless, it was not possible to intersect this fault. Probably, the fault dips to the west and therefore escapes drilling as it deepens. Borehole SC14 shows very low Lugeon permeabilities throughout. No major hydrogeological degradation is anticipated at this level. The limestone flank, on the other hand, can be more disturbed and permeable.

There is a good correlation between low resistivity and low velocity for line 1 corresponding to alluvium

Fig. 7. *Inverted section of line 1 at the left bank of the Wadi*
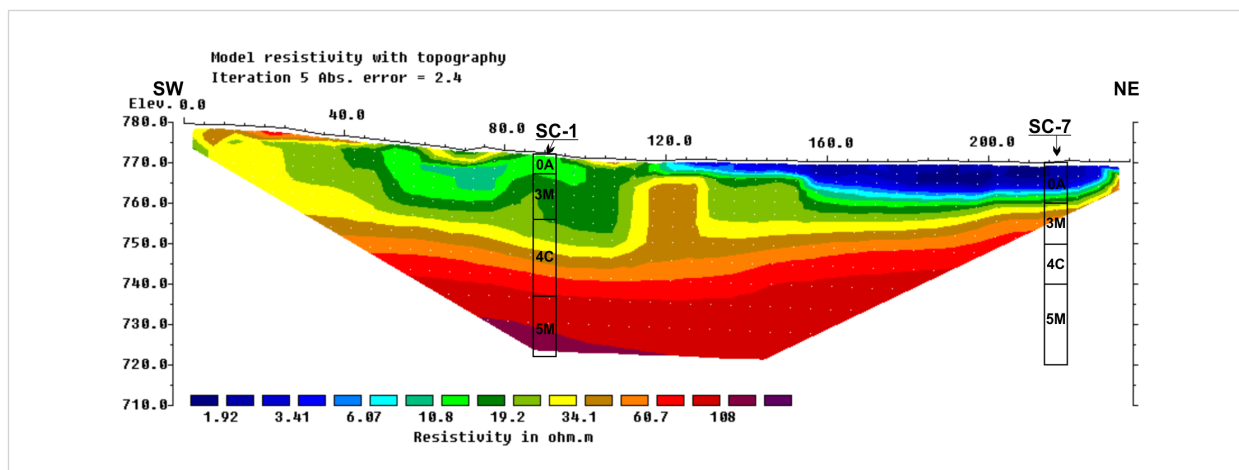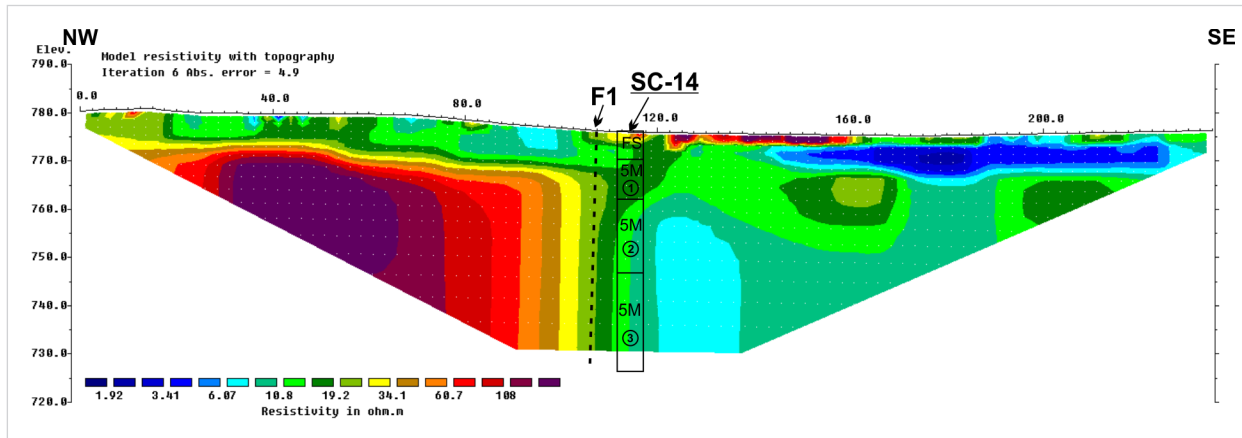
Fig. 8. *Inverted section of line 2 at the eastern part of the study area*

0A; however, the seismic refraction method detected two distinct layers: a shallow layer with low velocities (less than 520 m/s) and a deep layer with velocities reaching 1300 m/s. For the upper part of the section, the correlation between low resistivity and low velocity areas could be interpreted as zones composed of alluvium (0A).

Thus, the combination of ERT and seismic refraction on lines 1 and 2 improved the geological section by correlating scattered information from the boreholes in continuous 2D models representing the variations of resistivities and seismic velocities as a function of the depth.

Geotechnics

For a better characterization of the dam site from a geotechnical point of view, RQD (Rock Quality Designation) and Lugeon permeability tests were carried out from one bank to the other of the Wadi. The geotechnical section obtained, based on the lithological correlation between the four boreholes (*Fig. 9*), shows at the right of each borehole, respectively, the Lugeon

Fig. 9. *Geotechnical section showing Lugeon test permeability and RQD values (see Fig. 1 for section location)*
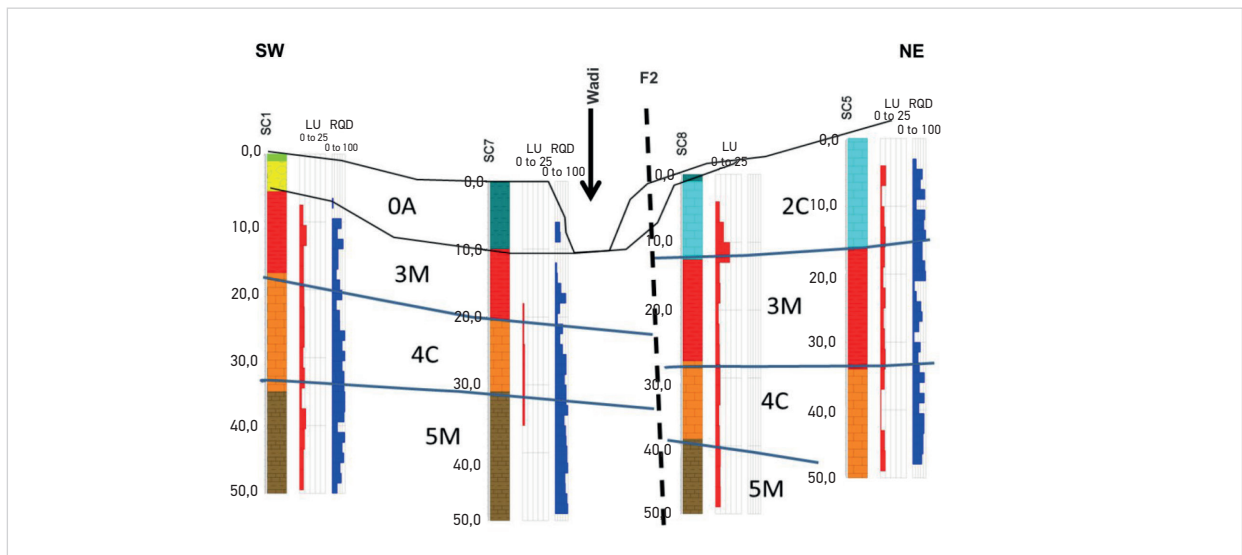
(Lu) permeability (red colour) and RQD values (blue colour). High Lugeon values are mainly encountered in 2C and 4C limestones (between 5 and 15 Lu) due to fracturing which affects them close to the surface, and very secondarily the 3M marls (between 2 and 5 Lu) when they are close to the surface and decompressed. Locally, some high values are encountered in the 5M marls, which remain very insignificant. At depth, the values are under 2 Lu and tend towards 0 Lu.

The examination of the RQD values shows that the low values are distributed irregularly between the boreholes. However, it is noted that in the vicinity of the F2 fault, the borehole SC8 presents globally lower RQD values. The F2 fault deduced from surface geology was confirmed by the drilling due to the shifts in the layers. From the correlation of the four boreholes, the F2 fault is a normal fault as is indicated by the shift of the formations 3M, 4C at the right bank of the Wadi.

Conclusions

At the end of this article and in the light of the results obtained from the various investigation techniques carried out on the dam site, the contribution of geophysics in the identification and characterization of the geology of the site seems very interesting. These different techniques made it possible, on the basis of the correlation with boreholes, to highlight the different lithological horizons, their extension and the limit between cover and bedrock.

There is a significant potential for infill materials in the basin of the future dam as revealed by VES and ERT data which show a near surface conductive electrical horizon that correlates with clays. Electric Resistivity Tomography by the contrast of the resistivity values made it possible to specify the structural aspect and identify the exact position of F1 fault at the east of the site. The combination of ERT and seismic refraction on lines 1 and 2 improved the geological section by correlating scattered information from the boreholes in continuous 2D models representing the variations of resistivities and seismic velocities as a function of depth. The normal F2 fault deduced from surface geology was confirmed by drilling due to shift of the formations 3M and 4C at the right bank of the Wadi.

Alluvial deposits that fill the valley correspond to lacustrine-type deposits and therefore set up within a water body. There was at a remote time a natural basin probably closed either at the level of the site or further downstream in which the fine sediments were deposited in a very uniform way. It is concluded that the basin area has already functioned as a lake, which is encouraging for its watertightness.

References

ANBT (2018) Etude d'Avant-Projet Détaillé du Barrage de Chebabta. Mission 3: Etude géologique, géotechnique et de sismicité [Detailed Preliminary Design Study of the Chebabta Dam. Mission 3: Geological, geotechnical and seismicity study] (in French).

Benson RC, Kaufmann RD, Yuhr L, Martin D. (1998). Assessment, prediction and remediation of karst conditions on I-70, Frederick, MD. In Proceedings of the 49th Highway Geology Symposium, 1998 September, 10-14; Prescott, Arizona. p. 313-325.

Bobachev, C. (2002). IPI2Win: A windows software for an automatic interpretation of resistivity sounding data , Ph.D. thesis, Moscow State University, Russia

Boubaya, D. (2017). Combining Resistivity and Aeromagnetic Geophysical Surveys for Groundwater Exploration in the Maghnia Plain of Algeria. Journal of Geological Research. Volume 2017, 1- 14 https://doi.org/10.1155/2017/1309053

Fehdi, C., Baali F., Boubaya, D., Rouabhia, A. (2011). Detection of sinkholes using 2D electrical resistivity imaging in the Cheria Basin (north-east of Algeria). Arabian Journal of Geosciences , 4,181-187. https://doi.org/10.1007/s12517-009-0117-2

Gouasmia, M., Mhamdi, A. , Chekhma, H., Lahmadi, M. , Amri,

F and Ben Dhia, H. (2007). Étude géophysique du site du barrage d'Oum Laksab (Tunisie Centre-Ouest). Revue Française de Géotechnique. N° 118, pp. 37-42 [Geophysical Study of Oum Laksab Dam site (Tunisian Central West)] (in French) https://doi.org/10.1051/geotech/2007118037

Lagabrielle. R. 2007. Géophysique appliquée au génie civil. Technique de l'ingénieur, traité Construction [Applied geophysics for civil engineering. in French]

Loke, M.H., 2002. Tutorial: 2-D and 3-D electrical imaging surveys. Geotomo software. https://www.geotomosoft.com/

Loke, M.H. and Barker, R.D. (1996). Rapid Least-Squares Inversion of Apparent Resistivity Pseudosections by a Quasi-Newton Method. Geophysical Prospecting, 44, 131-152. https://doi.org/10.1111/j.1365-2478.1996.tb00142.x

Mahleb, A., Hadji, R., Zahri, F., Boujellal ,R.,Chibani, A. and Hamad, Y.(2002). Water-Borne Erosion Estimation Using the Revised Universal Soil Loss Equation (RUSLE) Model Over a Semiarid Watershed: Case Study of Meskiana Catchment, Algerian-Tunisian Border. Geotech Geol Eng 40, 4217-4230. https://doi.org/10.1007/s10706-022-02152-3

Mouici, R., Baali, F, Hadji, T, Boubaya, D, Audra, P, Fehdi, C, Cailhol, D, Jaillet, S, Arfib, B. (2017). Geophysical, Geotechnical, And Speleologic Assessment For Karst-Sinkhole Collapse Genesis in Cheria Plateau (NE ALGERIA). Mining Science, vol. 24, 2017, 59–71.

Reynolds, J. M. (2011). An Introduction to Applied and Environmental Geophysics. Second Edition. New York, NY: Wiley-Blackwell.

Sari, M., Seren, A., Alemdag, S. (2020). Determination of geological structures by geophysical and geotechnical techniques in Kırklartepe Dam Site (Turkey). Journal of Applied Geophysics V 182. https://doi.org/10.1016/j.jappgeo.2020.104174

Singh, S. B. ,Veeraiah, B. , Dhar, R. L. ,Prakash B. A. and Rani, M. T. (2011). Deep resistivity sounding studies for probing deep fresh aquifers in the coastal area of Orissa, India, Hydrogeology Journal, vol. 19, no. 2, pp. 355-366. https://doi.org/10.1007/s10040-010-0697-7

Summit XStream Pro user guide revision 03. (2015). (www.summit-system.de). DMT GmbH & Co. KG Am Technologiepark 1 45307 Essen, Germany.

W-geoosoft/ WinSism V10. (2004). Seismic Refraction Processing Software instruction manual. http://www.wgeosoft.ch. W_GeoSoft, Switzerland.

Yousfi, C. Douaifia, W. (2020). Étude géophysique par trainée électrique et sismique réfraction du barrage de Chebabta, Meskiana Wilaya d'Oum El-Bouaghi. Master, Université de Tébessa [Geophysical study of Chebabta dam using eleric profiling and seismic refraction] (in French).

Zhou, W., Beck, B.F. & Adams, A.L. (2002). Effective electrode array in mapping karst hazards in electrical resistivity tomography. Environmental Geology volume 42, pp 922-928. https://doi.org/10.1007/s00254-002-0594-z